Hindawi
Discrete Dynamics in Nature and Society
Volume 2022, Article ID 2751592, 10 pages
https://doi.org/10.1155/2022/2751592

Research Article

Benchmark Problems for the Numerical Schemes of the Phase-Field Equations

Youngjin Hwang,[1] Chaeyoung Lee,[1] Soobin Kwak,[1] Yongho Choi,[2] Seokjun Ham,[1] Seungyoon Kang,[1] Junxiang Yang,[3] and Junseok Kim [1]

[1]*Department of Mathematics, Korea University, Seoul 02841, Republic of Korea*
[2]*Department of Mathematics and Big Data, Daegu University, Gyeongsan-si Gyeongsangbuk-do 38453, Gyeongsan, Republic of Korea*
[3]*School of Computer Science and Engineering, Sun Yat-Sen University, Guangzhou 510275, China*

Correspondence should be addressed to Junseok Kim; cfdkim@korea.ac.kr

Received 28 November 2021; Accepted 4 January 2022; Published 21 January 2022

Academic Editor: Francisco R. Villatoro

In this study, we present benchmark problems for the numerical methods of the phase-field equations. To find appropriate benchmark problems, we first perform a linear stability analysis and then take a growth mode solution as the benchmark problem, which is closely related to the dynamics of the original governing equations. As concrete examples, we perform convergence tests of the numerical methods of the Allen–Cahn (AC) and Cahn–Hilliard (CH) equations using the proposed benchmark problems. The one- and two-dimensional computational experiments confirm the accuracy and efficiency of the proposed scheme as the benchmark problems.

1. Introduction

In this study, we present benchmark problems for the numerical schemes of the phase-field equations. Two famous phase-field models are chosen as examples. The first equation is the Allen–Cahn (AC) equation [1, 2]:

$$\phi_t(x,t) = -\frac{F'(\phi(x,t))}{\varepsilon^2} + \Delta\phi(x,t), \quad \text{for } x \in \Omega,\ t > 0. \tag{1}$$

with the Neumann boundary condition $\mathbf{n} \cdot \nabla\phi = 0$ on $\partial\Omega$, where $\mathbf{n}$ is the exterior normal vector to the domain boundary $\partial\Omega$. The phase-field $\phi(\mathbf{x}, t)$ is the difference between the concentrations of the two mixtures components, the free energy $F(\phi) = 0.25(\phi^2 - 1)^2$ is double-well potential, and ϵ is a positive constant related to the thickness of the interfacial transition layer. The second equation is the Cahn–Hilliard (CH) equation [3]:

$$\phi_t(\mathbf{x},t) = \Delta\left[F'(\phi(\mathbf{x},t)) - \epsilon^2\Delta\phi(\mathbf{x},t)\right], \quad \text{for } \mathbf{x} \in \Omega,\ t > 0. \tag{2}$$

with the Neumann boundary condition $\mathbf{n} \cdot \nabla\phi = \mathbf{n} \cdot \nabla \cdot \Delta\phi = 0$ on $\partial\Omega$. Because there are no closed-form analytic solutions for the general initial and boundary conditions of the AC and CH equations, it is required to approximate the solutions of the equations using numerical methods. Therefore, to validate the accuracy of the newly proposed numerical methods, it is essential to test the developed methods with benchmark problems. The logarithmic Flory–Huggins potential is one of the useful potentials among phase-field models. In [4], the authors developed an appropriate temporal discretization method for the nonlinear term of the fourth-order CH equation with concentration dependent mobility and logarithmic Flory–Huggins potentials. The developed Invariant Energy Quadratization (IEQ) method is linear and unconditionally stable. Shen

et al. [5] proposed a scalar auxiliary variable (SAV) approach based on the IEQ method to construct accurate and efficient time discretization methods for a large class of gradient flows. Yang et al. [6] developed an improved SAV approach inspired by a step-by-step solving scheme based on the SAV approach for gradient flow problems which includes the AC and CH equations [7]. The improved SAV approach has all the advantages of classical SAV approach, further simplifies the algorithm, and easily constructs the temporally first-order and second-order methods. To solve the AC equation with Flory–Huggins potential, a novel energy factorization approach is used based on a stabilization technique called the stabilized energy factorization approach [8]. The discrete maximum principle and unconditional energy stability of the novel energy factorization approach have been rigorously proved using the discrete variational principle. A novel linear, energy stable, and maximum principle preserving scheme was developed to semi-implicitly treat double-well potentials in the AC equation using the energy factorization approach [9]. A variety of benchmark problems have been proposed for the phase-field models and used to validate the numerical schemes. Jokisaari et al. [10] proposed two benchmark problems: solute diffusion and second-phase growth and coarsening. Jeong et al. [11] presented two benchmark problems, which are shrinking annulus and spherical shell. They considered the CH equation in radially and spherically symmetric forms to obtain simple benchmark solutions. For the AC and CH equations, Church et al. [12] provided four benchmark problems. Zhang et al. [13] tested a class of linear numerical schemes for the functionalized CH equation using stabilized scalar auxiliary variable (SAV) method. Wu et al. [14] presented two benchmark problems on homogeneous and heterogeneous nucleation. Li et al. [15] suggested the numerical benchmark solution of the CH equation. They adopted the fourth-order Runge–Kutta method and finite difference method for the integration in time and the spatial differential operator, respectively, with a cosine initial condition. Hug et al. [16] proposed a benchmark problem for brittle fracture.

For example, Jeong et al. [11] used the following initial state for a benchmark problem:

$$\phi(r,0) = \tan h\left(\frac{0.1 - \mid r - 0.75 \mid}{\sqrt{2}\,\varepsilon}\right). \tag{3}$$

In [12], the authors used the following four benchmark problems:

$$\phi(x,0) = \cos(2x) + 0.01e^{\cos(x+0.1)}, \tag{4}$$

$$\phi(x,y,0) = 0.05\left[\cos(3x)\cos(4y) + \cos^2(4x)\cos^2(3y) + \cos(x-5y)\cos(2x-y)\right], \tag{5}$$

$$\phi(x,y,0) = \tan h\frac{\sqrt{(x-\pi)^2 + (y-\pi)^2} - 2}{\sqrt{2}\varepsilon}, \tag{6}$$

$$\phi(x,y,0) = -1 + \sum_{i=1}^{7} f\left(\sqrt{(x-x_i)^2 + (y-y_i)^2} - r\right)_i, \tag{7}$$

where $f(s) = 2e^{-e^2/s^2}$ if $s < 0$ and $f(s) = 0$ otherwise. In [13], the authors used the following initial condition for the benchmark problem:

$$\phi(x,y,0) = 2e^{\sin x + \sin y - 2} + 2.2e^{-\sin x - \sin y - 2} - 1. \tag{8}$$

Figure 1 shows some of the initial conditions for the benchmark problems.

However, most of the previous benchmark problems for the phase-field equations are chosen without any concrete theoretical basis. In [17], the authors developed a mathematical model including heat equation and optimization of the experimental parameters and temperature profiles, and the mathematical model was validated according to the numerical results without suggesting a benchmark problem. Benchmark problems with concrete theoretical basis are an important basis for validating the accuracy of mathematical models and numerical methods.

In this paper, we propose appropriate benchmark problems to verify the accuracy of the numerical methods based on the theoretical basis through linear stability analysis using simple initial conditions. First, we perform a linear stability analysis and then take a growth mode solution [18] as the benchmark problem, which is closely related to the dynamics of the original governing equations.

The layout of this paper is as follows. In Section 2, the procedure of finding benchmark problems is described. In Section 3, the numerical experiments are performed. In Section 4, the conclusions are given.

2. Proposed Benchmark Problems

In this section, the proposed benchmark problems are presented for the numerical methods of the one- and two-dimensional AC and CH phase-field models. We first conduct a linear stability analysis and then take a growth mode solution as the benchmark problem, which is closely related to the dynamics of the AC equation or the CH equation.

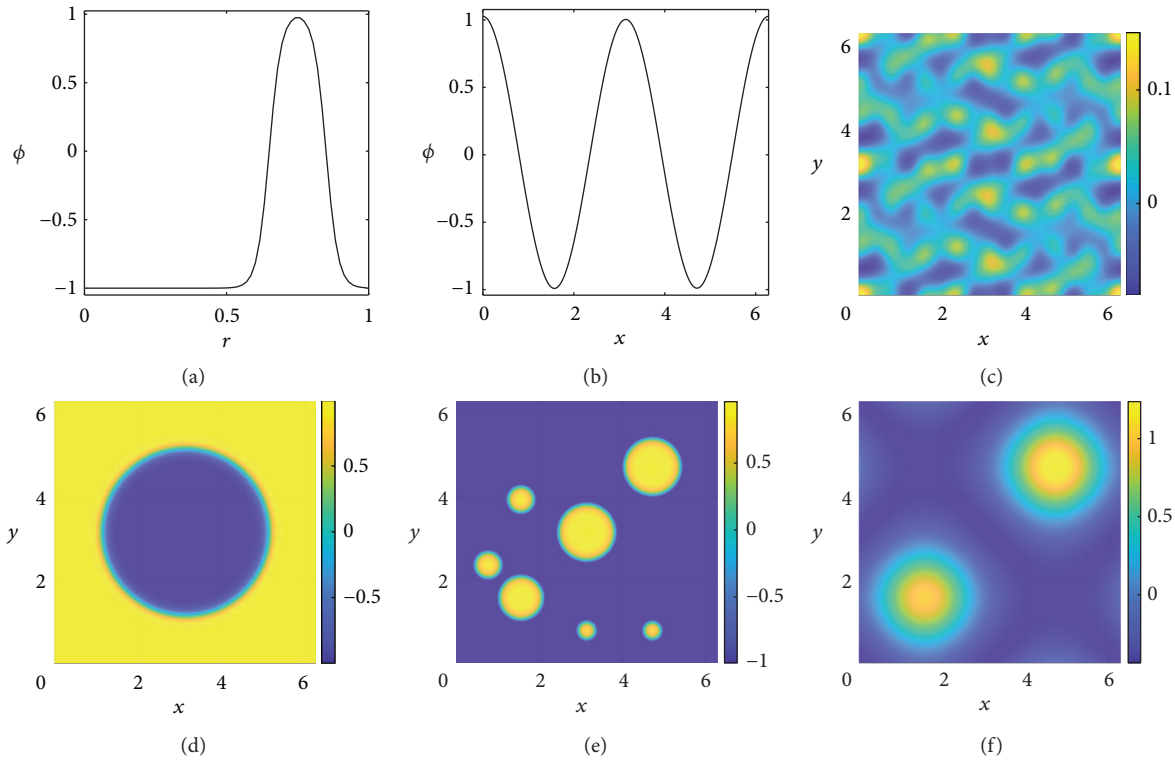

Figure 1: (a–f) The different initial conditions for benchmark problems from equations (3) to (8), respectively.

2.1. Benchmark Problems for the AC Equation. First, let us consider the benchmark problems for the one- and two-dimensional AC equation.

2.1.1. One-Dimensional AC Equation. The one-dimensional AC equation is as follows:

$$\phi_t(x,t) = -\frac{\phi^3(x,t) - \phi(x,t)}{\varepsilon^2} + \phi_{xx}(x,t), \quad \text{for } x \in \Omega = (0, 2\pi), t > 0. \tag{9}$$

with the Neumann boundary condition $\phi_x(0,t) = \phi_x(2\pi,t) = 0$. To find appropriate benchmark problems for the AC equation, a linear stability analysis is first conducted around a spatially constant critical composition solution $\phi = 0$. We linearize the nonlinear term $F'(\phi) = \phi^3 - \phi$ by applying the Taylor expansion and then get linearized term $F'(\phi) \approx -\phi$. Therefore, the linearized AC equation is as follows:

$$\phi_t(x,t) = \frac{\phi(x,t)}{\varepsilon^2} + \phi_{xx}(x,t). \tag{10}$$

For a positive integer k, we take $\Phi(x,t) = \alpha(t)\cos(kx)$ as a solution for (10), where $\alpha(t)$ is an amplitude. Substituting above $\Phi(x,t)$ into (10), we have

$$\alpha'(t)\cos(kx) = \frac{\alpha(t)\cos(kx)}{\varepsilon^2} - k^2\alpha(t)\cos(kx). \tag{11}$$

Dividing $\cos(kx)$ on the both sides of (11), we obtain

$$\alpha'(t) = \left(\frac{1}{\varepsilon^2} - k^2\right)\alpha(t). \tag{12}$$

Then, the solution of the ordinary differential equation (ODE) (12) is as follows:

$$\alpha(t) = \alpha(0)\exp\left[\left(\frac{1}{\varepsilon^2} - k^2\right)t\right]. \tag{13}$$

Let

$$\Phi(x,t) = \alpha(t)\cos(kx). \tag{14}$$

Be a benchmark problem solution for a one-dimensional modified AC equation, where $\alpha(t)$ is given by (13). Here, $\Phi(x,0) = \alpha(0)\cos(kx)$ is the initial condition. Next, when performing the convergence tests for the numerical schemes of the AC equation, we consider the following modified AC equation with a source term:

$$\phi_t(x,t) = -\frac{F'(\phi(x,t))}{\epsilon^2} + \phi_{xx}(x,t) + s(x,t) \quad \text{for } t > 0, \tag{15}$$

where

$$s(x,t) = \Phi_t(x,t) + \frac{F'(\Phi(x,t))}{\epsilon^2} - \Phi_{xx}(x,t) = \left[\alpha'(t) + \frac{1}{\epsilon^2}\left(\alpha^3(t)\cos^2(kx) - \alpha(t)\right) + k^2\alpha(t)\right]\cos(kx). \tag{16}$$

Here, the value of $\alpha(t)$ is given in (13) and $\alpha'(t)$ can be found by taking the first derivative of $\alpha(t)$ with respect to t. Note that if k is chosen to satisfy $k < 1/\varepsilon$, then the numerical solution grows as time evolves as seen from (13).

2.1.2. Two-Dimensional AC Equation. The two-dimensional AC equation is as follows:

$$\phi_t(x,y,t) = -\frac{\phi^3(x,y,t) - \phi(x,y,t)}{\varepsilon^2} + \Delta\phi(x,y,t),$$
$$\text{for } (x,y) \in \Omega = (0,2\pi)\times(0,2\pi),\ t>0. \tag{17}$$

with the Neumann boundary condition $\mathbf{n}\cdot\nabla\phi = 0$ on $\partial\Omega$, where $\mathbf{n}$ is the exterior normal vector to the domain boundary $\partial\Omega$. To find appropriate benchmark problems for the two-dimensional AC equation, we first conduct a linear stability analysis around a spatially constant critical composition solution $\phi = 0$. The nonlinear term $F'(\phi) = \phi^3 - \phi$ is linearized by applying the Taylor expansion, and then the linearized term $F'(\phi) \approx -\phi$ is obtained. Therefore, the linearized AC equation is as follows:

$$\phi_t(x,y,t) = \frac{\phi(x,y,t)}{\epsilon^2} + \phi_{xx}(x,y,t) + \phi_{yy}(x,y,t). \tag{18}$$

For positive integers k_x and k_y, let us consider $\Phi(x,y,t) = \alpha(t)\cos(k_x x)\cos(k_y y)$ as a two-dimensional benchmark solution for (18), where $\alpha(t)$ is an amplitude. Substituting above $\Phi(x,y,t)$ into (18), then

$$\alpha'(t)\cos(k_x x)\cos(k_y y) = \frac{\alpha(t)\cos(k_x x)\cos(k_y y)}{\epsilon^2} - \left(k_x^2 + k_y^2\right)\alpha(t)\cos(k_x x)\cos(k_y y). \tag{19}$$

Dividing $\cos(k_x x)\cos(k_y y)$ on the both sides of (19), we obtain

$$\alpha'(t) = \left(\frac{1}{\epsilon^2} - k_x^2 - k_y^2\right)\alpha(t). \tag{20}$$

Then, the solution of the ODE (19) is as follows:

$$\alpha(t) = \alpha(0)\exp\left[\left(\frac{1}{\varepsilon^2} - k_x^2 - k_y^2\right)t\right]. \tag{21}$$

Let

$$\Phi(x,y,t) = \alpha(t)\cos(k_x x)\cos(k_y y). \tag{22}$$

be a benchmark problem solution for the modified AC equation, where $\alpha(t)$ is given by (21). The initial condition is given by $\Phi(x,y,0) = \alpha(0)\cos(k_x x)\cos(k_y y)$. Finally, when we perform convergence tests for numerical schemes of the AC equation, the following modified AC equation with a source term is taken:

$$\phi_t(x,y,t) = -\frac{F'(\phi(x,y,t))}{\varepsilon^2} + \Delta\phi(x,y,t) + s(x,y,t),$$
$$\text{for } (x,y) \in \Omega, t>0, \tag{23}$$

where

$$s(x,y,t) = \Phi_t(x,y,t) + \frac{F'(\Phi(x,y,t))}{\varepsilon^2} - \Delta\Phi(x,y,t)$$
$$= \left[\alpha'(t) + \frac{1}{\varepsilon^2}\left(\alpha^3(t)\cos^2(k_x x)\cos^2(k_y y) - \alpha(t)\right) + \left(k_x^2 + k_y^2\right)\alpha(t)\right]\cos(k_x x)\cos(k_y y). \tag{24}$$

Here, the value of $\alpha(t)$ is given in (21) and $\alpha'(t)$ can be found by taking the first derivative of $\alpha(t)$ with respect to t. Note that if we set k_x and k_y satisfying $k_x^2 + k_y^2 < 1/\varepsilon^2$, then the numerical solution grows as time evolves as seen from (21).

2.2. Benchmark Problems for the CH Equation. Next, let us consider the benchmark problems for the one- and two-dimensional CH equation.

2.2.1. One-Dimensional CH Equation. The one-dimensional CH equation is as follows:

$$\phi_t(x,t) = \left[\phi^3(x,t) - \phi(x,t) - \epsilon^2\phi_{xx}(x,t)\right]_{xx},$$
$$\text{for } x \in \Omega = (0,2\pi), t>0. \tag{25}$$

with the Neumann boundary condition $\phi_x(0,t) = \phi_x(2\pi,t) = \phi_{xxx}(0,t) = \phi_{xxx}(2\pi,t) = 0$. Similar to the benchmark problem solution of the AC equation, a linear stability analysis is first conducted around a spatially

constant critical composition solution $\phi = 0$. Then, the linearized CH equation is as follows:

$$\phi_t(x,t) = -\phi_{xx}(x,t) - \epsilon^2\phi_{xxxx}(x,t). \tag{26}$$

For the positive integer k, we consider $\Phi(x,t) = \beta(t)\cos(kx)$ as a solution for (26), where $\beta(t)$ is an amplitude. Substituting above $\Phi(x,t)$ into (26), we have

$$\beta'(t)\cos(kx) = k^2\beta(t)\cos(kx) - k^4\epsilon^2\beta(t)\cos(kx). \tag{27}$$

Dividing $\cos(kx)$ on the both sides of (27), we obtain

$$\beta'(t) = k^2\left[1 - (k\epsilon)^2\right]\beta(t). \tag{28}$$

Then, the solution of the ODE (28) is as follows:

$$\beta(t) = \beta(0)\exp\left[k^2\left(1 - (k\epsilon)^2\right)t\right]. \tag{29}$$

Let

$$\Phi(x,t) = \beta(t)\cos(kx). \tag{30}$$

be a benchmark problem solution for the CH equation, where $\beta(t)$ is given by (29). The initial condition is given by $\Phi(x,0) = \beta(0)\cos(kx)$. Finally, to conduct convergence tests for numerical schemes of the CH equation, the following modified CH equation with a source term is considered:

$$\begin{aligned}\phi_t(x,t) = &\left[F'(\phi(x,t)) - \epsilon^2\phi_{xx}(x,t)\right]_{xx}\\ &+ s(x,t) \quad \text{for } t > 0,\end{aligned} \tag{31}$$

where

$$\begin{aligned}s(x,t) &= \Phi_t(x,t) - \left[F'(\Phi(x,t)) - \epsilon^2\Phi_{xx}(x,t)\right]_{xx}\\ &= \left[\beta'(t) + \frac{3k^2\beta^3(t)}{4} - k^2\beta(t) + k^4\epsilon^2\beta(t)\right]\cos(kx)\\ &\quad + \frac{9k^2\beta^3(t)}{4}\cos(3kx),\end{aligned} \tag{32}$$

where the triple angle identity for cosine is applied, that is, $\cos^3(kx) = [\cos(3kx) + 3\cos(kx)]/4$. Here, the value of $\beta(t)$ is given in (29) and $\beta'(t)$ can be found by taking the first derivative of $\beta(t)$ with respect to t. Note that if k is chosen to satisfy $k < 1/\varepsilon$, then the numerical solution grows as time evolves as seen from (29).

2.2.2. Two-Dimensional CH Equation. The two-dimensional CH equation is as follows:

$$\begin{aligned}&\phi_t(x,y,t) = \Delta\left[\phi^3(x,y,t) - \phi(x,y,t) - \varepsilon^2\Delta\phi(x,y,t)\right],\\ &\text{for } (x,y) \in \Omega = (0,2\pi)\times(0,2\pi), t > 0.\end{aligned} \tag{33}$$

With the Neumann boundary condition $\mathbf{n}\cdot\nabla\phi = 0$ on $\partial\Omega$, where $\mathbf{n}$ is the exterior normal vector to the domain boundary $\partial\Omega$. A linear stability analysis is conducted around a spatially constant critical composition solution $\phi = 0$. Then, the linearized CH equation is as follows:

$$\phi_t(x,y,t) = \Delta\left[-\phi(x,y,t) - \epsilon^2\Delta\phi(x,y,t)\right]. \tag{34}$$

For the positive integers k_x and k_y, $\Phi(x,y,t) = \beta(t)\cos(k_x x)\cos(k_y y)$ is given as a solution for (34), where $\beta(t)$ is an amplitude. Substituting above $\Phi(x,y,t)$ into (34), we have

$$\beta'(t)\cos(k_x x)\cos(k_y y) = \left(k_x^2 + k_y^2\right)\left[1 - \left(k_x^2 + k_y^2\right)\epsilon^2\right]\beta(t)\cos(k_x x)\cos(k_y y). \tag{35}$$

Dividing $\cos(k_x x)\cos(k_y y)$ on the both sides of (35), we obtain

$$\beta'(t) = \left(k_x^2 + k_y^2\right)\left[1 - \left(k_x^2 + k_y^2\right)\epsilon^2\right]\beta(t). \tag{36}$$

Then, the solution of the ODE (36) is as follows:

$$\beta(t) = \beta(0)\exp\left[\left(k_x^2 + k_y^2\right)\left[1 - \left(k_x^2 + k_y^2\right)\epsilon^2\right]t\right]. \tag{37}$$

Let

$$\Phi(x,y,t) = \beta(t)\cos(k_x x)\cos(k_y y), \tag{38}$$

be a benchmark problem solution for the CH equation, where $\beta(t)$ is given by (37). The initial condition is given by $\Phi(x,y,0) = \beta(0)\cos(k_x x)\cos(k_y y)$. Finally, when conducting convergence tests for the numerical schemes of the

CH equation, we consider the following modified CH equation with a source term:

$$\phi_t(x,y,t) = \Delta\left[F'(\phi(x,y,t)) - \epsilon^2\Delta\phi(x,y,t)\right] + s(x,y,t), \quad (39)$$

where

$$\begin{aligned} s(x,y,t) &= \Phi_t(x,y,t) - \Delta\left[F'(\Phi(x,y,t)) - \varepsilon^2\Delta\Phi(x,y,t)\right] \\ &= \frac{\beta^3(t)}{16}\left[3\cos(k_x x)\cos\left(3k_y y\right)\left(k_x^2 + 9k_y^2\right) + 3\cos(3k_x x)\cos\left(k_y y\right)\left(9k_x^2 + k_y^2\right)\right] \\ &\quad +9\cos(k_x x)\cos\left(k_y y\right)\left(k_x^2 + k_y^2\right) + 9\cos(3k_x x)\cos\left(3k_y y\right)\left(k_x^2 + k_y^2\right)\Big] \\ &\quad +\left(\beta'(t) - \beta(t)\left(1 - \varepsilon^2\left(k_x^2 + k_y^2\right)\right)\right)\left(k_x^2 + k_y^2\right)\cos(k_x x)\cos\left(k_y y\right). \end{aligned} \quad (40)$$

Here, the value of $\beta(t)$ is given in (37) and $\beta'(t)$ can be found by taking the first derivative of $\beta(t)$ with respect to t. Note that if k_x and k_y are given satisfying $k_x^2 + k_y^2 < 1/\varepsilon^2$, then the numerical solution grows as time evolves as seen from (37).

3. Numerical Experiments

In this section, we compute the numerical solutions of the two phase-field equations and verify the accuracy of the proposed method. A multigrid algorithm [19–21] is used to solve the discrete equations. Let the l_2 -norm errors (l_2-error) be defined as $\|\mathbf{e}_{N_x}^{N_t}\|_2 = \sqrt{1/N_x\sum_{i=1}^{N_x}(e_i^{N_t})^2}$, where $e_i^{N_t} = \phi_i^{N_t} - \Phi(x_i,T)$ for $i = 1,\ldots,N_x$ in one-dimensional space, and $\|\mathbf{e}_{N_x,N_y}^{N_t}\|_2 = \sqrt{1/N_xN_y\sum_{i=1}^{N_x}\sum_{j=1}^{N_y}(e_{ij}^{N_t})^2}$, where $e_{ij}^{N_t} = \phi_{ij}^{N_t} - \Phi(x_i,y_j,T)$ for $i = 1,\ldots,N_x$, $j = 1,\ldots,N_y$ in two-dimensional space.

3.1. Convergence Test for One-Dimensional AC Equation. A convergence test of the proposed method is conducted for the one-dimensional AC equation. Let ϕ_i^n be approximation of $\phi(x_i,t_n)$, where $x_i = (i-0.5)h$, $i = 1,2,\ldots,N_x$ and $h = 2\pi/N_x$. Equation (1) is discretized by applying the θ -method [22] as follows:

$$\begin{aligned} \frac{\phi_i^{n+1} - \phi_i^n}{\Delta t} &= (1-\theta)\left(-\frac{(\phi_i^n)^3 - \phi_i^n}{\varepsilon^2} + \Delta_h\phi_i^n\right) \\ &\quad + \theta\left(-\frac{\left(\phi_i^{n+1}\right)^3 - \phi_i^{n+1}}{\varepsilon^2} + \Delta_h\phi_i^{n+1}\right) + s_i^{n+1/2}, \end{aligned} \quad (41)$$

where $\Delta_h\phi_i^n = (\phi_{i-1}^n - 2\phi_i^n + \phi_{i+1}^n)/h^2$. Here, if $\theta = 0.5$, then (41) is the Crank–Nicolson (CN) method [23]; else if $\theta = 1$, then it is the fully implicit Euler method. The Neumann boundary condition is applied, thus, $\phi_0^n = \phi_1^n$ and $\phi_{N_x+1}^n = \phi_{N_x}^n$ for all $n = 0,1,\ldots$. The discretized (41) is solved by using the multigrid algorithm. The nonlinear part $(\phi_i^{n+1})^3$ of $F'(\phi_i^{n+1})$ is linearized at ϕ_i^m, therefore, $(\phi_i^{n+1})^3 \approx (\phi_i^m)^3 + 3(\phi_i^m)^2(\phi_i^{n+1} - \phi_i^m)$. Here, m is the Gauss–Seidel relaxation step in the multigrid algorithm.

The initial condition is $\phi(x,0) = 0.2\cos(2x)$ on $\Omega = (0,2\pi)$, thus, $\Phi(x,T) = 0.2e^{(1/\varepsilon^2-4)T}\cos(2x)$ on $\Omega = (0,2\pi)$ is a benchmark problem solution for the AC equation. The multigrid algorithm parameters are set as follows: the number of Gauss–Seidel relaxation iteration = 3, the tolerance = 1.0*e* -8, and the maximum number of iteration = 300.

3.1.1. Fully Implicit Method. Table 1 shows the convergence test results of the fully implicit method ($\theta = 1$) for time step, with $T = 1.0e-5$ and various temporal step sizes $\Delta t = T/N_t$ where $N_t = 8, 16, 32$, and 64. Other parameters are fixed as follows: $N_x = 2048$, $h = 2\pi/N_x$, and $\varepsilon = h$.

Table 2 shows the convergence test results of the fully implicit method for space step, with $T = 1.0e-5$ and various spatial step sizes $h = 2\pi/N_x$ where $N_x = 8, 16, 32$, and 64. Other parameters are fixed as follows: $N_t = 2048$, $\Delta t = T/N_t$, and $\varepsilon = \pi/32$.

3.1.2. Crank–Nicolson Method. Table 3 shows the convergence test results of the CN method ($\theta = 0.5$) for time step, with $T = 1.0e$ -5 and various temporal step sizes $\Delta t = T/N_t$ where $N_t = 8, 16, 32$, and 64. Other parameters are fixed as follows: $N_x = 2048$, $h = 2\pi/N_x$, and $\varepsilon = h$.

Table 4 shows the convergence test results of the CN method for space step, with $T = 1.0e$ -5 and various spatial step sizes $h = 2\pi/N_x$ where $N_x = 8, 16, 32$, and 64. Other parameters are fixed as follows: $N_t = 2048$, $\Delta t = T/N_t$, and $\varepsilon = \pi/32$.

3.2. Convergence Test for Two-Dimensional AC Equation. Let ϕ_i^n be approximation of $\phi(x_i,y_j,t_n)$, where $x_i = (i-0.5)h$, $i = 1,2,\ldots,N_x$, $y_j = (j-0.5)h$, $j = 1,2,\ldots,N_y$ and $h = 2\pi/N_x = 2\pi/N_y$. The

Table 1: Convergence test results of the fully implicit method for time step.

Case	$(h, \Delta t)$	Rate	$(h, \Delta t/2)$	Rate	$(h, \Delta t/4)$	Rate	$(h, \Delta t/8)$
l_2-error	1.6730e-2	1.02	8.2512e-3	1.01	4.0976e-3	1.00	2.0419e-3

Table 2: Convergence test results of the fully implicit method for space step.

Case	$(h, \Delta t)$	Rate	$(h/2, \Delta t)$	Rate	$(h/4, \Delta t)$	Rate	$(h/8, \Delta t)$
l_2-error	1.0727e-6	1.91	2.8517e-7	1.98	7.2424e-8	1.99	1.8199e-8

Table 3: Convergence test results of the CN method for time step.

Case	$(h, \Delta t)$	Rate	$(h, \Delta t/2)$	Rate	$(h, \Delta t/4)$	Rate	$(h, \Delta t/8)$
l_2-error	3.5295e-4	1.99	8.8705e-5	2.00	2.2206e-5	2.00	5.5533e-6

Table 4: Convergence test results of the CN method for space step.

Case	$(h, \Delta t)$	Rate	$(h/2, \Delta t)$	Rate	$(h/4, \Delta t)$	Rate	$(h/8, \Delta t)$
l_2-error	1.0726e-6	1.91	2.8514e-7	1.98	7.2393e-8	1.99	1.8168e-8

two-dimensional AC equation is discretized by applying the θ -method as follows:

$$\frac{\phi_{ij}^{n+1}-\phi_{ij}^{n}}{\Delta t}=(1-\theta)\left(-\frac{F'\left(\phi_{ij}^{n}\right)}{\varepsilon^2}+\Delta_h\phi_{ij}^{n}\right)+\theta\left(-\frac{F'\left(\phi_{ij}^{n+1}\right)}{\varepsilon^2}+\Delta_h\phi_{ij}^{n+1}\right)+s_{ij}^{n+1/2}, \tag{42}$$

where $0\le\theta\le 1$, $\Delta_h\phi_{ij}^{n}=(\phi_{i+1}^{n}+\phi_{i-1}^{n}+\phi_{i,j+1}^{n}+\phi_{i,j-1}^{n}-4\phi_{ij}^{n})/h^2$. We set the ghost points as $\phi_{0,j}^{n}=\phi_{1,j}^{n}$, $\phi_{N_x+1,j}^{n}=\phi_{N_x,j}^{n}$, $j=1,2,\ldots,N_y$ and $\phi_{i,0}^{n}=\phi_{i,1}^{n}$, $\phi_{i,N_y+1}^{n}=\phi_{i,N_y}^{n}$, $i=1,2,\ldots,N_x$ for all $n=0,1,\ldots$, because the Neumann boundary condition is adopted. The discretized governing equation is solved by using the multigrid method.

The initial condition is $\phi(x,y,0)=0.2\cos(2x)\cos(2y)$ on $\Omega=(0,2\pi)\times(0,2\pi)$, thus, $\Phi(x,y,T)=0.2e^{(1/\varepsilon^2-8)T}\cos(2x)\cos(2y)$ on $\Omega=(0,2\pi)\times(0,2\pi)$ is the benchmark problem solution for the two-dimensional AC equation. The multigrid algorithm parameters are taken as follows: the number of Gauss–Seidel relaxation iteration = 3, the tolerance = 1.0e -8, and the maximum number of iteration = 300.

3.2.1. Fully Implicit Method. Table 5 shows the convergence test results of the fully implicit method for time step, with T = 1.0e -5 and various temporal step sizes $\Delta t = T/N_t$ where N_t = 8, 16, 32, and 64. Other parameters are fixed as follows: $N_x = N_y$ = 2048, $h = 2\pi/N_x$, and $\varepsilon = h$.

Table 5: Convergence test results of the fully implicit method for time step.

Case	$(h, \Delta t)$	Rate	$(h, \Delta t/2)$	Rate	$(h, \Delta t/4)$	Rate	$(h, \Delta t/8)$
l_2-error	1.4487e-2	1.04	7.0306e-3	1.02	3.4646e-3	1.01	1.7199e-3

Table 6 shows the convergence test results of the fully implicit method for space step, with T = 1.0e -5 and various spatial step sizes $h = 2\pi/N_x = 2\pi/N_y$ where $N_x = N_y$ = 8, 16, 32, and 64. Other parameters are fixed as follows: N_t = 2048, $\Delta t = T/N_t$, and $\varepsilon = \pi/32$.

3.2.2. Crank–Nicolson Method. Table 7 shows the convergence test results of the CN method for time step, with T = 1.0e -5 and various temporal step sizes $\Delta t = T/N_t$ where N_t = 8, 16, 32, and 64. Other parameters are fixed as follows: $N_x = N_y$ = 2048, $h = 2\pi/N_x$, and $\epsilon = h$.

Table 8 shows the convergence test results of the CN method for space step, with T = 1.0e -5 and various spatial step sizes $h = 2\pi/N_x$ where N_x = 8, 16, 32, and 64. Other parameters are fixed as follows: N_t = 2048, $\Delta t = T/N_t$, and $\varepsilon = \pi/32$.

It is demonstrated that the calculated numerical results are appropriate benchmark problems for verifying the correctness of the numerical methods for the AC equation.

3.3. Convergence Test for One-Dimensional CH Equation. We consider the convergence tests of numerical schemes for CH equation. Equation (2) is discretized by applying the nonlinearly convex splitting method [24] as follows:

$$\frac{\phi_i^{n+1}-\phi_i^{n}}{\Delta t}=\Delta_h\mu_i^{n+1},\ \mu_i^{n+1}=\left(\phi_i^{n+1}\right)^3-\phi_i^{n}-\epsilon^2\Delta_h\phi_i^{n+1}+s_i^{n+\frac{1}{2}}, \tag{43}$$

where $i=1,2,\ldots,N_x$. Here, the ghost points are set as $\phi_0^n=\phi_1^n$, $\phi_{Nx+1}^n=\phi_{Nx}^n$, $\mu_0^n=\mu_1^n$ and $\mu_{Nx+1}^n=\mu_{Nx}^n$ for all $n=0,1,\ldots$, because the Neumann boundary condition is applied. The multigrid algorithm is used to solve (43)

The initial condition is $\phi(x,0)=0.2\cos(2x)$ on $\Omega=(0,2\pi)$, thus, $\Phi(x_i,T)=0.2e^{(4-16\epsilon^2)T}\cos(2x)$ on $\Omega=(0,2\pi)$ is the benchmark problem solution for the CH equation. The multigrid algorithm parameters are set as follows: the number of Gauss–Seidel relaxation iteration = 3, the tolerance = 1.0e -8, and the maximum number of iteration = 100.

Table 9 shows the convergence test results of the unconditionally stable method [25] for time step, with T = 1.0e -2 and various temporal step sizes $\Delta t = T/N_t$ where N_t = 8, 16, 32, and 64. Other parameters are fixed as follows: N_x = 2048, $h = 2\pi/N_x$, and $\varepsilon = 8h$.

Table 10 shows the convergence test results of the unconditionally stable method for space step, with T = 1.0e -2 and various spatial step sizes $h = 2\pi/N_x$ where

Table 6: Convergence test results of the fully implicit method for space step.

Case	$(h, \Delta t)$	Rate	$(h/2, \Delta t)$	Rate	$(h/4, \Delta t)$	Rate	$(h/8, \Delta t)$
l_2-error	1.5169e-6	1.91	4.0326e-7	1.98	1.0240e-7	1.99	2.5714e-8

Table 7: Convergence test results of the CN method for time step.

Case	$(h, \Delta t)$	Rate	$(h, \Delta t/2)$	Rate	$(h, \Delta t/4)$	Rate	$(h, \Delta t/8)$
l_2-error	2.1410e-4	2.00	5.3658e-5	2.00	1.3423e-5	2.00	3.3562e-6

Table 8: Convergence test results of the CN method for space step.

Case	$(h, \Delta t)$	Rate	$(h/2, \Delta t)$	Rate	$(h/4, \Delta t)$	Rate	$(h/8, \Delta t)$
l_2-error	1.5169e-6	1.91	4.0324e-7	1.98	1.0238e-7	1.99	2.5693e-8

Table 9: Convergence test results of the unconditionally stable method for time step.

Case	$(h, \Delta t)$	Rate	$(h, \Delta t/2)$	Rate	$(h, \Delta t/4)$	Rate	$(h, \Delta t/8)$
l_2-error	1.6655e-5	1.00	8.3544e-6	1.00	4.1886e-6	0.99	2.1017e-6

Table 10: Convergence test results of the unconditionally stable method for space step.

Case	$(h, \Delta t)$	Rate	$(h/2, \Delta t)$	Rate	$(h/4, \Delta t)$	Rate	$(h/8, \Delta t)$
l_2-error	1.4948e-3	2.10	3.4801e-4	1.88	9.4222e-5	1.97	2.4093e-05

$N_x = 8, 16, 32$, and 64. Other parameters are fixed as follows: $N_t = 2048$, $\Delta t = T/N_t$, and $\varepsilon = \pi/32$.

3.4. Convergence Test for Two-Dimensional CH Equation. Next, the two-dimensional CH equation is also discretized by applying the nonlinearly convex splitting method as follows:

$$\frac{\phi_{ij}^{n+1} - \phi_{ij}^{n}}{\Delta t} = \Delta_h \mu_{ij}^{n+1}, \mu_{ij}^{n+1} = \left(\phi_{ij}^{n+1}\right)^3 - \phi_{ij}^{n} - \varepsilon^2 \Delta_h \phi_{ij}^{n+1} + s_{ij}^{n+1/2}, \tag{44}$$

where $i = 1, 2, \ldots, N_x$, $j = 1, 2, \ldots, N_y$. The ghost points are set as $\phi_{0,j}^n = \phi_{1,j}^n$, $\phi_{Nx+1,j}^n = \phi_{Nx,j}^n$, $\mu_{0,j}^n = \mu_{1,j}^n$, $\mu_{Nx+1,j}^n = \mu_{Nx,j}^n$, $j = 1, 2, \ldots, Ny$ and $\phi_{i,0}^n = \phi_{i,1}^n$, $\phi_{i,Nx+1}^n = \phi_{i,Nx}^n$, $\mu_{i,0}^n = \mu_{i,1}^n$, $\mu_{i,Nx+1}^n = \mu_{i,Nx}^n$, $i = 1, 2, \ldots, Nx$, for all $n = 1, 2, \ldots$, because of the Neumann boundary condition. The multigrid algorithm is used to solve (44)

The initial condition is $\phi(x, y, t) = 0.2\cos(2x)\cos(2y)$ on $\Omega = (0, 2\pi) \times (0, 2\pi)$, thus $\Phi(x, y, T) = 0.2e^{(8-64\varepsilon^2)T}\cos(2x)\cos(2y)$ on $\Omega = (0, 2\pi) \times (0, 2\pi)$ is the benchmark problem solution for the CH equation. The multigrid algorithm parameters are taken as follows: the number of Gauss–Seidel relaxation iteration = 3, the tolerance = 1.0*e* -8, and the maximum number of iteration = 100.

Table 11 shows the convergence test results of the unconditionally stable method for time step, with $T = 1.0e$ -2 and various temporal step sizes $\Delta t = T/N_t$ where $N_t = 8, 16, 32$, and 64. Other parameters are fixed as follows: $N_x = N_y = 2048$, $h = 2\pi/N_x$, and $\varepsilon = 8h$.

Table 12 shows the convergence test results of the unconditionally stable method for space step, with $T = 1.0e$ -2 and various spatial step sizes $h = 2\pi/N_x = 2\pi/N_y$ where $N_x = N_y = 8, 16, 32$, and 64. Other parameters are fixed as follows: $N_t = 2048$, $\Delta t = T/N_t$, and $\varepsilon = \pi/32$.

It is demonstrated that the calculated numerical results are appropriate benchmark problems for verifying the correctness of the nonlinear convex splitting method for the CH equation.

3.5. Convergence Test for Two-Dimensional CH Equation Based the SAV Approach. The two-dimensional CH equation is discretized by applying the SAV approach [5]. The SAV approach is a step-by-step solving approach, and it can achieve both temporally first- and second-order accuracy. In this section, we consider the first-order SAV approach and perform the convergence test. For a detailed description of the SAV approach, see [5]. First, we define a time-dependent variable U as $U(t) = \sqrt{\int_\Omega F(\phi)\mathrm{d}x}$, $F(\phi) = 0.25(\phi^2 - 1)^2$.

Next, let $\phi^{n+1} = \overline{\phi}^{n+1} + U^{n+1}\widehat{\phi}^{n+1}$, $\mu^{n+1} = \overline{\mu}^{n+1} + U^{n+1}\widehat{\mu}^{n+1}$. Therefore, we can rewrite (44) as

$$\frac{\overline{\phi}^{n+1} - \phi^{n}}{\Delta t} = \Delta \overline{\mu}^{n+1} + s_{ij}^{n+1/2}, \overline{\mu}^{n+1} = -\varepsilon^2 \Delta \overline{\phi}^{n+1} + S\left(\overline{\phi}^{n+1} - \phi^{n}\right), \tag{45}$$

$$\frac{\widehat{\phi}^{n+1}}{\Delta t} = \Delta \widehat{\mu}^{n+1}, \widehat{\mu}^{n+1} = -\epsilon^2 \Delta \widehat{\phi}^{n+1} + \frac{F'(\phi^n)}{\sqrt{\int_\Omega F(\phi^n)\mathrm{d}\mathbf{x}}} + S\widehat{\phi}^{n+1}, \tag{46}$$

where $i = 1, 2, \ldots, N_x$, $j = 1, 2, \ldots, N_y$ and S is a positive constant that plays a role of stabilization. The ghost points are set as $\overline{\phi}_{0,j}^n = \overline{\phi}_{1,j}^n$, $\overline{\phi}_{N_x+1,j}^n = \overline{\phi}_{N_x,j}^n$, $\overline{\mu}_{0,j}^n = \overline{\mu}_{1,j}^n$, $\overline{\mu}_{N_x+1,j}^n = \overline{\mu}_{N_x,j}^n$, $j = 1, 2, \ldots, N_y$ and $\overline{\phi}_{i,0}^n = \overline{\phi}_{i,1}^n$, $\overline{\phi}_{i,N_x+1}^n = \overline{\phi}_{i,N_x}^n$, $\overline{\mu}_{i,0}^n = \overline{\mu}_{i,1}^n$, $\overline{\mu}_{i,N_x+1}^n = \overline{\mu}_{i,N_x}^n$, $i = 1, 2, \ldots, N_x$ for all $n = 1, 2, \ldots$, and ghost points for $\widehat{\phi}^n$, $\widehat{\mu}^n$ are set similarly to $\overline{\phi}^n$, $\overline{\phi}^n$, respectively. The multigrid algorithm is used to solve CH equation with SAV approach. We use $\phi(x, y, 0) = 0.2\cos(2x)\cos(2y)$ on $\Omega = (0, 2\pi) \times (0, 2\pi)$, therefore $\Phi(x, y, T) = 0.2e^{(8-64\epsilon^2)T}\cos(2x)\cos(2y)$ on $\Omega = (0, 2\pi) \times (0, 2\pi)$ is the benchmark problem solution for the CH equation and stabilization constant is $S = 2$. The multigrid algorithm parameters are taken as follows: the number of Gauss–Seidel relaxation iteration = 3, the tolerance = 1.0*e* -8, and the maximum number of iteration = 100.

Table 13 shows the first-order convergence test results of the SAV approach for time step, with $T = 1.0e$ -2 and various

Table 11: Convergence test results of the unconditionally stable method for time step.

Case	$(h, \Delta t)$	Rate	$(h, \Delta t/2)$	Rate	$(h, \Delta t/4)$	Rate	$(h, \Delta t/8)$
l_2-error	9.5984e-2	0.99	4.8199e-2	1.00	2.4169e-2	1.00	1.2119e-2

Table 12: Convergence test results of the unconditionally stable method for space step.

Case	$(h, \Delta t)$	Rate	$(h/2, \Delta t)$	Rate	$(h/4, \Delta t)$	Rate	$(h/8, \Delta t)$
l_2-error	1.7444e-3	2.08	4.1116e-4	1.93	1.0805e-4	1.98	2.7467e-5

Table 13: Convergence test results of the SAV approach for time step.

Case	$(h, \Delta t)$	Rate	$(h, \Delta t/2)$	Rate	$(h, \Delta t/4)$	Rate	$(h, \Delta t/8)$
l_2-error	1.3104e-03	0.98	6.6381e-04	0.99	3.3418e-04	0.99	1.6772e-04

Table 14: Convergence test results of the SAV approach for space step.

Case	$(h, \Delta t)$	Rate	$(h/2, \Delta t)$	Rate	$(h/4, \Delta t)$	Rate	$(h/8, \Delta t)$
l_2-error	1.0963e-02	2.08	2.5863e-03	1.92	6.8208e-04	1.96	1.7592e-04

temporal step sizes $\Delta t = T/N_t$, where $N_t = 8, 16, 32$, and 64. Other parameters are fixed as follows: $N_x = N_y = 2048$, $h = 2\pi/N_x$, and $\epsilon = 8h$.

Table 14 shows the second-order convergence test results of the SAV approach for space step, with $T = 1.0e$ -2 and various spatial step sizes $h = 2\pi/N_x = 2\pi/N_y$ where $N_x = N_y = 8, 16, 32$, and 64. Other parameters are fixed as follows: $N_t = 2048$, $\Delta t = T/N_t$, and $\varepsilon = \pi/32$.

It is demonstrated that the calculated numerical experiment results are appropriate benchmark problems for verifying the convergence rates of the SAV approach for the CH equation.

4. Conclusion

In this study, a benchmark problem is presented for the numerical technique of phase-field equations. To show the effectiveness of the proposed method, two famous phase-field equations were considered. To design an appropriate benchmark problem for the AC equation and the CH equation on the one- and two-dimensional, we first performed a linear stability analysis and then took a growth mode solution as the benchmark problem, which is closely related to the dynamics of the original governing equation. For each phase-field equation, convergence tests were conducted of the numerical schemes. The computational results confirmed the accuracy and efficiency of the proposed method. The proposed method is general; therefore, it is possible to design benchmark problems for various phase-field equations or directly extend to higher dimensions such as three-dimensional space.

Data Availability

The data used to support the findings of this study are included in the article.

Conflicts of Interest

The authors declare that they have no conflicts of interest.

Acknowledgments

The first author (Y. Hwang) was supported by the National Research Foundation (NRF), Korea, under project BK21 FOUR. The corresponding author (J. S. Kim) was supported by Korea University Grant.

References

[1] S. M. Allen and J. W. Cahn, "A microscopic theory for antiphase boundary motion and its application to antiphase domain coarsening," *Acta Metallurgica*, vol. 27, no. 6, pp. 1085–1095, 1979.

[2] D. Lee and S. Lee, "Image segmentation based on modified fractional Allen–Cahn equation," *Mathematical Problems in Engineering*, vol. 2019, Article ID 3980181, 6 pages, 2019.

[3] J. W. Cahn and J. E. Hilliard, "Free energy of a nonuniform system. I. Interfacial free energy," *The Journal of Chemical Physics*, vol. 28, no. 2, pp. 258–267, 1958.

[4] X. Yang and J. Zhao, "On linear and unconditionally energy stable Algorithms for variable mobility Cahn–Hilliard type equation with logarithmic flory–huggins potential," *Communications in Computational Physics*, vol. 25, no. 3, pp. 703–728, 2019.

[5] J. Shen, J. Xu, and J. Yang, "The scalar auxiliary variable (SAV) approach for gradient flows," *Journal of Computational Physics*, vol. 353, pp. 407–416, 2018.

[6] J. Yang and J. Kim, "An improved scalar auxiliary variable (SAV) approach for the phase-field surfactant model," *Applied Mathematical Modelling*, vol. 90, pp. 11–29, 2021.

[7] Z. Liu and X. Li, "Step-by-step solving schemes based on scalar auxiliary variable and invariant energy quadratization approaches for gradient flows," *Numerical Algorithms*, vol. 89, pp. 1–22, 2021.

[8] X. Wang, J. Kou, and J. Cai, "Stabilized energy factorization approach for Allen–Cahn equation with logarithmic Flory–Huggins potential," *Journal of Scientific Computing*, vol. 82, no. 2, pp. 1–23, 2020.

[9] X. Wang, J. Kou, and H. Gao, "Linear energy stable and maximum principle preserving semi-implicit scheme for Allen–Cahn equation with double well potential,"

Communications in Nonlinear Science and Numerical Simulation, vol. 98, Article ID 105766, 14 pages, 2021.

[10] A. M. Jokisaari, P. W. Voorhees, J. E. Guyer, J. Warren, and O. G. Heinonen, "Benchmark problems for numerical implementations of phase field models," *Computational Materials Science*, vol. 126, pp. 139–151, 2017.

[11] D. Jeong, Y. Choi, and J. Kim, "A benchmark problem for the two- and three-dimensional Cahn-Hilliard equations," *Communications in Nonlinear Science and Numerical Simulation*, vol. 61, pp. 149–159, 2018.

[12] J. M. Church, Z. Guo, P. K. Jimack et al., "High accuracy benchmark problems for allen-Cahn and Cahn-Hilliard dynamics," *Communications in Computational Physics*, vol. 26, no. 4, pp. 947–972, 2019.

[13] C. Zhang, J. Ouyang, C. Wang, and S. M. Wise, "Numerical comparison of modified-energy stable SAV-type schemes and classical BDF methods on benchmark problems for the functionalized Cahn–Hilliard equation," *Journal of Computational Physics*, vol. 423, Article ID 109772, 35 pages, 2020.

[14] W. Wu, D. Montiel, J. E. Guyer et al., "Phase field benchmark problems for nucleation," *Computational Materials Science*, vol. 193, Article ID 110371, 11 pages, 2021.

[15] Y. Li, C. Lee, J. Wang, S. Yoon, J. Park, and J. Kim, "A simple benchmark problem for the numerical methods of the Cahn–Hilliard equation," *Discrete Dynamics in Nature and Society*, vol. 2021, Article ID 8889603, 8 pages, 2021.

[16] L. Hug, S. Kollmannsberger, Z. Yosibash, and E. Rank, "A 3D benchmark problem for crack propagation in brittle fracture," *Computer Methods in Applied Mechanics and Engineering*, vol. 364, Article ID 112905, 17 pages, 2020.

[17] Y. Xu, Y. Liu, and L. Zhang, "Effects of the solder phase transformation on the optimization of reflow soldering parameters and temperature profiles," *Discrete Dynamics in Nature and Society*, vol. 2021, Article ID 9955967, 19 pages, 2021.

[18] Y. Li, D. Jeong, H. Kim, C. Lee, and J. Kim, "Comparison study on the different dynamics between the Allen-Cahn and the Cahn-Hilliard equations," *Computers & Mathematics with Applications*, vol. 77, no. 2, pp. 311–322, 2019.

[19] U. Trottenberg, C. W. Oosterlee, and A. Schuller, *Multigrid*, Academic Press, New York, 2000.

[20] J. Kim, "A numerical method for the Cahn-Hilliard equation with a variable mobility," *Communications in Nonlinear Science and Numerical Simulation*, vol. 12, no. 8, pp. 1560–1571, 2007.

[21] Y. Wang and Y. Ge, "High-Order compact difference scheme and multigrid method for solving the 2D elliptic problems," *Mathematical Problems in Engineering*, vol. 2018, Article ID 7831731, 11 pages, 2018.

[22] W. Zhou, "Application of FDM and FEM in solving the simultaneous heat and moisture transfer inside bread during baking," *International Journal of Computational Fluid Dynamics*, vol. 19, no. 1, pp. 73–77, 2005.

[23] J. Crank and P. Nicolson, "A practical method for numerical evaluation of solutions of partial differential equations of the heat-conduction type," *Mathematical Proceedings of the Cambridge Philosophical Society*, Cambridge University Press, vol. 43, no. 1, pp. 50–67, 1947.

[24] H. G. Lee, J. Shin, and J.-Y. Lee, "A high-order convex splitting method for a non-additive Cahn-Hilliard energy functional," *Mathematics*, vol. 7, no. 12, Article ID 1242, 2019.

[25] J. Yang and J. Kim, "An unconditionally stable second-order accurate method for systems of Cahn–Hilliard equations," *Communications in Nonlinear Science and Numerical Simulation*, vol. 87, Article ID 105276, 17 pages, 2020.